

# Bifurcation of Axons from Cranial Sensory Neurons Is Disabled in the Absence of Npr2-Induced cGMP Signaling

Gohar Ter-Avetisyan, Fritz G. Rathjen, and Hannes Schmidt

Max Delbrück Center for Molecular Medicine, 13092 Berlin, Germany

Axonal branching is a prerequisite for the establishment of complex neuronal circuits and their capacity for parallel information processing. Previously, we have identified a cGMP signaling pathway composed of the ligand C-type natriuretic peptide (CNP), its receptor, the guanylyl cyclase natriuretic peptide receptor 2 (Npr2), and the cGMP-dependent kinase I $\alpha$  (cGKI $\alpha$ ) that regulates axon bifurcation of dorsal root ganglion (DRG) neurons in the spinal cord. Now we asked whether this cascade also controls axon bifurcation elsewhere in the nervous system. An Npr2-lacZ reporter mouse line was generated to clarify the pattern of the CNP receptor expression. It was found that during the period of axonal outgrowth, Npr2 and cGKI $\alpha$  were strongly labeled in neurons of all cranial sensory ganglia (gV, gVII, gVIII, gIX, and gX). In addition, strong complementary expression of CNP was detected in the hindbrain at the entry zones of sensory afferents. To analyze axon branching in individual Npr2-positive neurons, we generated a mouse mutant expressing a tamoxifen-inducible variant of Cre recombinase expressed under control of the Npr2-promoter (Npr2-CreER<sup>T2</sup>). After crossing this strain with conditional reporter mouse lines, we revealed that the complete absence of Npr2 activity indeed prohibited the bifurcation of cranial sensory axons in their entrance region. Consequently, axons only turned in either an ascending or descending direction, while collateral formation and growth of the peripheral arm was not affected. These findings indicate that in neurons of the cranial sensory ganglia, as in DRG neurons, cGMP signals are necessary for the execution of an axonal bifurcation program.

**Key words:** axonal branching; cGKI; cGMP signaling; CNP; cranial sensory ganglia; Npr2

## Introduction

Axonal branching enables an individual neuron to connect with distinct targets, thereby providing a framework for the parallel processing of neural signals in the CNS. Impairments of programs that trigger axonal branching might result in functional alterations (Schmidt and Rathjen, 2010; Gallo, 2011; Gibson and Ma, 2011; Lewis et al., 2013).

Dorsal root ganglion (DRG) neurons projecting into the spinal cord already proved to be an attractive system for the molecular analysis of axon branching. Intracellular labeling of DRG neurons has shown that after entering the spinal cord, sensory afferents exhibit axonal branching of first, second, and higher order (Brown, 1981). At the first axonal branch point in the cord,

DRG axons bifurcate in the dorsal column into two stem axons, which proceed further in the rostrocaudal plane. From the stem, axons bud numerous ventrally directed collaterals that in turn form higher-order branches (Ozaki and Snider, 1997; Schmidt and Rathjen, 2010).

The molecular mechanisms controlling the bifurcation of the main axon and collateral formation at the second-order branch point appear to be fundamentally different (Schmidt and Rathjen, 2010; Gallo, 2011). A cGMP signaling cascade composed of C-type natriuretic peptide (CNP), the receptor guanylyl cyclase Npr2 (also known as GC-B or Npr-B), and the cGMP-dependent kinase I $\alpha$  (cGKI $\alpha$ , also termed PKGI $\alpha$ ) regulates the first-order bifurcation of DRG axons in the dorsal column. In the absence of any of these components, sensory axons no longer bifurcate and instead form solitary stem axons that turn in either the rostral or caudal direction (Schmidt et al., 2002, 2007, 2009; Zhao and Ma, 2009; Zhao et al., 2009). Factors implicated in collateral formation of DRG axons are currently unknown, while terminal branching is regulated by SAD (synapses of amphids defective) kinases (Lilley et al., 2013).

A major open question was to what extent the mechanism underlying the bifurcation of DRG afferents in the spinal cord can be generalized. To obtain a reliable answer, it was necessary to provide information on the molecular basis of axon bifurcation in the hindbrain. Specifically, we aimed to investigate whether CNP-induced cGMP signaling also controls bifurcation of sensory afferents from the cranial ganglia, which develop from a different source than spinal ganglia (Lleras-Forero and Streit,

Received Sept. 30, 2013; revised Nov. 18, 2013; accepted Nov. 23, 2013.

Author contributions: G.T.-A., F.G.R., and H.S. designed research; G.T.-A. and H.S. performed research; G.T.-A. and H.S. analyzed data; G.T.-A., F.G.R., and H.S. wrote the paper.

This work was supported by Deutsche Forschungsgemeinschaft Grants SFB665 and FOR2060. We are grateful to Drs. Rosemarie Grantyn (Charité, Berlin, Germany) and Alistair Garratt (Max Delbrück Center for Molecular Medicine) for critical reading of the manuscript. We thank Dr. Hagen Wende, Andrea Leschke (both Max Delbrück Center for Molecular Medicine), and the transgenic core facility of the Max Delbrück Center for Molecular Medicine for their help during the generation of the Npr2-lacZ and the Npr2-CreER<sup>T2</sup> mutant mice; Dr. Sylvia Arber (Friedrich Miescher Institute, Basel, Switzerland) for providing the tau-mGFP strain; Madlen Driesner and Karola Bach for technical support; and Dr. Kira Balueva (Max Delbrück Center for Molecular Medicine) for the help with tamoxifen application.

The authors declare no competing financial interests.

Correspondence should be addressed to either of the following: Fritz G. Rathjen, Max Delbrück Center for Molecular Medicine, Robert Rössle Str. 10, 13092 Berlin, Germany. E-mail: rathjen@mdc-berlin.de; or Hannes Schmidt, Max Delbrück Center for Molecular Medicine, Robert Rössle Str. 10, 13092 Berlin, Germany. E-mail: hannes.schmidt@mdc-berlin.de.

DOI:10.1523/JNEUROSCI.4183-13.2014

Copyright © 2014 the authors 0270-6474/14/340737-11\$15.00/0

2012). For the analysis of the *Npr2* expression profile, we generated an *Npr2-lacZ* reporter mouse line. To clarify the impact of *Npr2*-induced cGMP signaling, we applied a genetic strategy for sparse labeling of *Npr2*-expressing neurons that involved the generation of a mouse mutant encoding a tamoxifen-inducible Cre recombinase under control of the *Npr2* promoter (*Npr2-CreER<sup>T2</sup>*; Feil et al., 1996; Rotolo et al., 2008).

By crossing this *Npr2-CreER<sup>T2</sup>* driver strain with reporter mouse lines, we revealed that the bifurcation of axons from neurons of all cranial sensory ganglia is impaired in the absence of *Npr2*. Thus, axons of cranial sensory neurons, which are similar to DRG neurons, use *Npr2*-induced cGMP signaling to trigger axon bifurcation in the hindbrain. We demonstrate that a cGMP-dependent signaling pathway controls first-order axon bifurcation but not higher-order branching of sensory neurons entering the CNS at any level.

## Materials and Methods

**Mice.** Animals were handled in accordance with protocols approved by the local animal use and care authority (LaGeSo, Berlin). The *Npr2-lacZ* mouse line was generated by standard procedures replacing exon 1 of the *Npr2* gene by a lacZ expression cassette with a nuclear localization sequence followed by a polyA stretch and a self-excising Cre recombinase cassette flanked by two loxP sites. The latter contains a testis-specific promoter as well as a neomycin resistance gene. A 10.4 kb fragment containing exons 1–3 of the *Npr2* gene was isolated and cloned by gap repair from BAC (bacterial artificial chromosome) clone bMQ331a20 (Source BioScience) for the generation of the targeting construct (Lee et al., 2001). Embryonic day (E) 14.1 ES cells (129/Ola) were electroporated and clones that had incorporated the targeting vector into their genome were selected by G418 and analyzed for homologous recombination after digestion with PstI by Southern blot analysis using a 5' probe amplified by primers 5'-TCATTTAATTTTCTGACTG-3' and 5'-TTACTTGTTTAGAAACAGG-3' and a 3' probe amplified by primers 5'-GTAA GCCAAGAAAGTGGGG-3' and 5'-GCAGACAGAGAGAAGGCATAG-3'. Blastocysts were injected and chimeras that transmitted the mutant *Npr2-lacZ* gene were identified by mating *Npr2<sup>lacZ/+</sup>* males to C57BL/6J females. Similarly, using the same BAC clone, the *Npr2-CreER<sup>T2</sup>* strain was generated by replacing exon 1 of the *Npr2* gene by coding sequences of the tamoxifen-inducible Cre recombinase (*CreER<sup>T2</sup>*; Feil et al., 1997) followed by a polyA stretch and a neomycin resistance gene flanked by FRT [FLP (flippase) recombinase target] sites. AB2.1 ES cells (129S7/SvEvBrd) were electroporated and screened by Southern blotting using the same probes as for the *Npr2-lacZ* mutant mouse. Subsequently, the neomycin segment was removed by crossbreeding with the FLP-deleter strain (B6.129S4-Gt(ROSA)26Sor<sup>tm1(FLP1)Dym</sup>/Rain); The Jackson Laboratories).

Other mouse lines used in this study were as follows: *Z/AP* (The Jackson Laboratory; Lobe et al., 1999), tau-mGFP (Hippenmeyer et al., 2005), *Npr2-cn* (The Jackson Laboratory; Tsuji and Kunieda, 2005), *cGKI* (Wegener et al., 2002), *CNP-lacZ* (Schmidt et al., 2009). Cross breeding of *Npr2-CreER<sup>T2</sup>* mice with reporter lines has been previously described in detail (Schmidt et al., 2013).

**Genotyping of *Npr2-lacZ* and *Npr2-CreER<sup>T2</sup>*.** Routine genotyping was performed by PCR amplification of genomic DNA isolated by the High Pure PCR Template Preparation Kit according to manufacturer's instructions (Roche). For the *Npr2-lacZ* strain, a 398 bp fragment of the *LacZ* allele and a 348 bp fragment of the wild-type allele were amplified using oligonucleotides P1 (5'-TGCCACCCTATCCTTAGTCC-3'), P2 (5'-GTGTTCTGGCAGCACCAC-3'), and P3 (5'-TCGCTATTACG CCAGCTG-3'). PCR analysis of the *Npr2-CreER<sup>T2</sup>* strain using oligonucleotides P4 (5'-CTCAGATTCCCTTCTCG-3'), P5 (5'-GGCATAGCT CAGTTGTGT-3'), and P6 (5'-TTGGACATGGTGAATTCAT-3') resulted in the amplification of a 356 bp fragment of the mutant allele and a 456 bp fragment of the wild-type allele.

**Tamoxifen administration.** To induce alkaline phosphatase (AP) expression in embryos containing the *Z/AP* reporter, tamoxifen was administered (0.1 mg/g body weight) by oral gavage to timed pregnant

animals at E9.5 as described previously (Joyner and Zervas, 2006). Embryos were collected at E12.5, E13.5, or E15.5 to analyze reporter expression in central projections and collaterals of *Npr2*-positive cranial sensory neurons. For recombination of the tau-mGFP reporter gene, 4-hydroxytamoxifen (Sigma-Aldrich) was prepared according to a previously described protocol (Indra et al., 1999) and administered (2 µg/g body weight) to timed pregnant mice at E9.5. GFP expression was analyzed in E12.5 embryos by immunostaining of 50 µm cryosections.

**Histology.** For whole-mount 5-bromo-4-chloro-3-indolyl-β-D-galactopyranoside (X-gal) staining, embryos were fixed in PBS containing 0.2% glutaraldehyde, 50 mM EGTA, pH 7.3, and 20 mM MgCl<sub>2</sub> at 4°C for 15–30 min, depending on the developmental stage. Tissues were then equilibrated in β-galactosidase (β-gal) wash solution (20 mM MgCl<sub>2</sub>, 0.02% Nonidet-P40, 0.01% sodium deoxycholate in PBS) and subsequently stained in β-gal wash solution containing 0.5 mg/ml X-gal and 5 mM potassium ferrocyanide and ferricyanide at room temperature or 37°C. After development of a blue color, the reaction was stopped by transferring the embryos to PBS containing 2 mM MgCl<sub>2</sub>. After two rounds of washing in PBS, the probes were postfixed in 4% paraformaldehyde and further processed for clearing before microscopic analysis.

For X-gal staining or immunohistochemical detection of β-gal in tissue sections, embryos were fixed in Zamboni's fixative (Stefanini et al., 1967) at room temperature for 30–90 min according to the developmental stage of the specimen. Following fixation, tissues were cryoprotected, embedded in OCT compound (Sakura Finetek), and sectioned at a thickness of 25 µm for X-gal staining or 15 µm for immunohistochemistry.

X-gal staining of frozen sections was done as described above for whole-mount embryos.

Detection of AP activity in parasagittal vibratome sections of *Npr2<sup>CreERT2/+</sup>;Z/AP<sup>+</sup>* or *Npr2<sup>CreERT2/cn</sup>;Z/AP<sup>+</sup>* mouse embryos was performed as previously described (Schmidt et al., 2013).

**Optical clearing.** X-gal-stained whole-mount embryo preparations were cleared in a solution containing 4 M urea, 10% (v/v) glycerol, and 0.1% (v/v) Triton X-100 for 3 weeks followed by incubation in a solution containing 8 M urea and 0.1% glycerol for 4 d at 4°C (Hama et al., 2011). The whole-mount embryos were further incubated in the first solution for 1–2 months, depending on embryonic age.

Vibratome sections processed for AP staining were dehydrated using a graded ethanol series [25, 50, 75, 100% (v/v)]. After dehydration, the sections were cleared in benzyl alcohol/benzyl benzoate (BABB; one part/two parts). After imaging, the sections were rehydrated and stored in PBS at 4°C.

**Immunohistochemistry, generation of antibodies, DiI labeling, and apoptosis detection.** Immunofluorescent staining and DiI labeling were performed as described previously (Schmidt et al., 2007; Schmidt and Rathjen, 2011). The following primary antibodies were used in combination with appropriate fluorophore-conjugated secondary antibodies: chicken anti-β-galactosidase (1:5000; Jackson ImmunoResearch), rabbit anti-β-gal (1:20,000; Cappel), rabbit anti-GFP (1:10,000; Jackson ImmunoResearch), mouse anti-neurofilament-M (7.5 µg/ml; 2H3, Developmental Hybridoma Bank), rabbit anti-Cre (1:10,000; Millipore), and rabbit anti-L1 (Rathjen and Schachner, 1984). Guinea pig anti-cGKIα (1:25,000) or guinea pig anti-Npr2 (1:10,000) have been generated to the N-terminal region of mouse cGKIα (amino acid residues 2–89) or to the extracellular region of mouse Npr2, respectively, by injections of the antigens at fortnightly intervals (Charles River).

Apoptosis was detected using TumorTACS *In Situ* Apoptosis Detection Kit (Trevigen) followed by standard eosin staining protocol. From each genotype, seven sagittal sections were analyzed for apoptosis and quantified.

**Image acquisition and analysis.** Images of whole-mount X-gal-processed embryos and of 250 µm vibratome sections stained for AP activity were obtained using a microscope (Axiovert 135) equipped with a charge-coupled device camera (AxioCam HRC) and acquisition software (AxioVision3.1; all from Carl Zeiss). Vibratome sections were imaged in BABB clearing solution in a 50 mm Lumox hydrophilic culture dish. Confocal images of immunohistochemical stainings and DiI-labeling experiments were captured with a Carl Zeiss LSM 710 NLO laser scanning microscope using ZEN 2010 software. The obtained data were

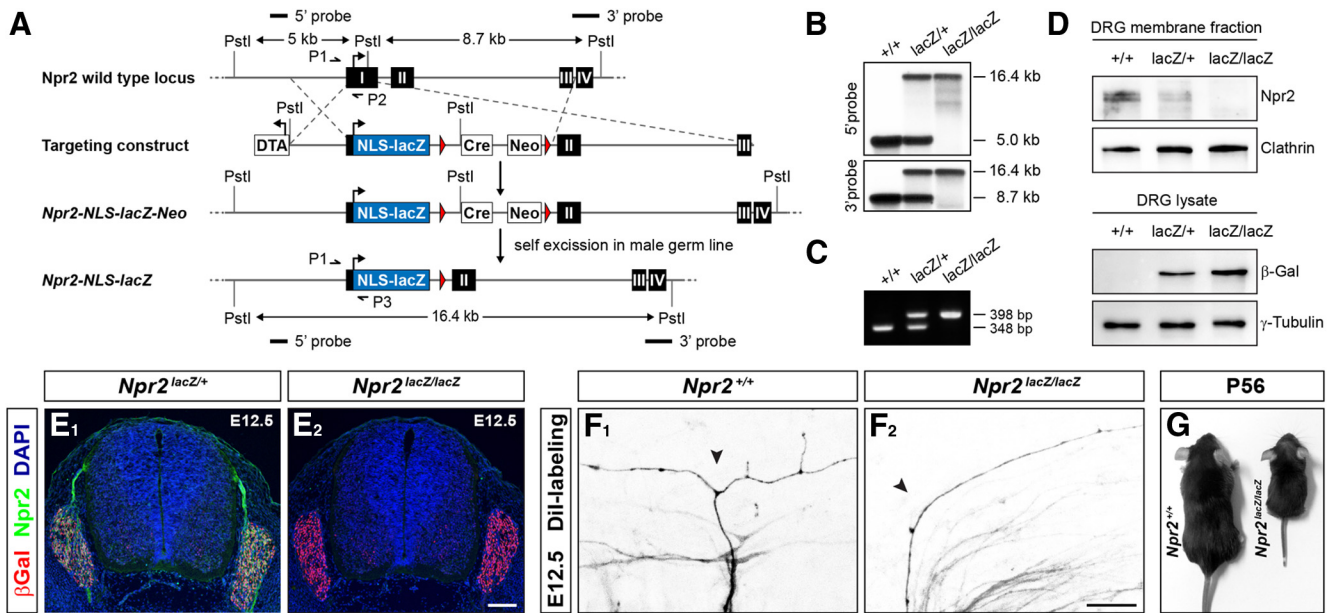


**Figure 1.** An *Npr2-lacZ* mouse strain as reporter of the *Npr2* expression profile. **A**, Targeting strategy for the generation of the *Npr2-lacZ* mouse line. **B–D**, Southern blot (**B**), PCR genotyping (**C**), and Western blot analyses (**D**) of wild-type, *Npr2<sup>lacZ/+</sup>*, and *Npr2<sup>lacZ/lacZ</sup>* mice. **E<sub>1</sub>**, **E<sub>2</sub>**, Immunohistochemical analysis of transverse sections of *Npr2<sup>lacZ/+</sup>* (**E<sub>1</sub>**) and *Npr2<sup>lacZ/lacZ</sup>* (**E<sub>2</sub>**) spinal cords at E12.5 using antibodies against  $\beta$ -gal and *Npr2* confirms the absence of *Npr2* expression in DRG neurons from *Npr2<sup>lacZ/lacZ</sup>* mice. Nuclei were visualized by DAPI stain. **F**, Dorsal views of Dil-labeled axons from DRG neurons from control and *Npr2<sup>lacZ/lacZ</sup>* embryos at E12.5 show a loss of axon bifurcation in *Npr2*-deficient animals. Fluorescence images are inverted. Lateral, bottom; caudal, left. **G**, Depiction of wild-type and *Npr2<sup>lacZ/lacZ</sup>* littermates at postnatal day 56, demonstrating a severely reduced body size in *Npr2*-deficient animals due to impaired endochondral ossification as described previously for other *Npr2* mutants (Tamura et al., 2004; Tsuji and Kunieda, 2005; Geister et al., 2013). Scale bars: **E**, 100  $\mu$ m; **F**, 25  $\mu$ m.

imported to the Adobe Photoshop CS4 software, cropped, and assembled in Adobe Illustrator CS3. The brightness and contrast were adjusted uniformly across entire images maintaining signal linearity and confirming that fluorescence intensity was not saturated.

**Quantification and statistical analysis.** For the colocalization study of *Npr2*, cGKI $\alpha$ , and neurofilament-M in cranial sensory ganglia, 15 horizontal cryosections from three mouse embryos were analyzed for each ganglion. Quantification of the triple immunostainings with DAPI counterstaining was done on the images of sections obtained by confocal laser scanning microscopy using a 40 $\times$  oil-immersion objective. The total number of the cells and the number of colocalized cells were counted in a 4000  $\mu$ m<sup>2</sup> field with an appropriate imaging channel and with simultaneous detection of 2-fluorescence or 3-fluorescence channels, respectively.

The size of the trigeminal funiculus was quantified in confocal images of transverse cryostat sections of littermate wild-type and *Npr2<sup>lacZ/lacZ</sup>* embryos labeled with an antiserum specific for cGKI $\alpha$  ( $\geq 60$  sections from three embryos from each genotype were measured) using the ImageJ 1.47q software (National Institutes of Health).

Apoptotic cells were quantified on seven serial sagittal sections of the trigeminal ganglion for each genotype by counting the number of dead cells (stained black) in an area of 25,000  $\mu$ m<sup>2</sup>.

The bifurcation behavior of individual cranial sensory axons was analyzed by counting AP-stained or GFP-labeled axons using light microscopy or confocal laser scanning microscopy, respectively.

## Results

### Coexpression of *Npr2* and cGKI $\alpha$ in all cranial sensory ganglia and complementary localization of CNP in axonal entry zones of the hindbrain

To identify candidate neuronal populations that might use *Npr2*-mediated cGMP signaling to trigger axon bifurcation, we generated a targeted *Npr2-lacZ* reporter mouse to study the expression profile of *Npr2* in the developing nervous system (Fig. 1A). Southern blot and PCR analysis indicated the correct integration of the target vector into the mouse genome (Fig. 1B,C). Western blotting and immunostainings show the absence of *Npr2* protein

in *Npr2-lacZ* homozygotes and the presence of  $\beta$ -gal in extracts or cryostat sections of embryonic DRGs (Fig. 1D–E). *Npr2<sup>lacZ/lacZ</sup>* mice lack the bifurcation of DRG axons at the dorsal root entry zone and develop a dwarfed phenotype as reported for the spontaneous *cn/cn* mutant mouse, which expresses an inactive form of *Npr2* due to a missense mutation (Fig. 1F–G; Tsuji and Kunieda, 2005; Schmidt et al., 2007). Together, these data indicated the correctness of the targeting strategy.

To correlate the expression of *Npr2* with the localization of CNP and cGKI $\alpha$  in embryonic whole mounts or cryostat sections, we used X-gal or immunostaining of *Npr2-lacZ* heterozygous mice. At E10.5, *Npr2* becomes strongly expressed in all cranial sensory ganglia (gV, gVII, gVIII, gIX, and gX) and in DRGs (Fig. 2A<sub>1</sub>–L<sub>1</sub>), which is consistent with *in situ* hybridization experiments in data bases (<http://www.eurexpress.org/>). In addition, *Npr2* was also detected at E10.5–E12.5 in the nasal region, in the mesencephalon, and at the midbrain–hindbrain border. Importantly, an overlapping expression pattern with *Npr2* in all cranial sensory ganglia was detected for cGKI $\alpha$  and neurofilament-M (Fig. 2M<sub>1</sub>–Q<sub>2</sub>; note that due to a nuclear localization signal,  $\beta$ -gal representing *Npr2* is detected in the nuclei of cells while antibody staining for cGKI $\alpha$  or neurofilament-M reveals a cytosolic distribution). About 75% of DAPI-positive cells coexpress *Npr2*, cGKI $\alpha$ , and neurofilament in the different cranial sensory ganglia (Fig. 2R). The remaining population of  $\sim 25\%$  of *Npr2*-negative, cGKI $\alpha$ -negative, and neurofilament-negative cells might be precursor or supporting cells. Except for small populations in ventral layers or in rhombomere 1, *Npr2* is not found in cells of the spinal cord or hindbrain, respectively, at the stages examined (Fig. 2D<sub>1</sub>–F<sub>1</sub>, H<sub>1</sub>–L<sub>1</sub>).

Furthermore, a strong complementary distribution of CNP, the ligand of *Npr2*, was observed at these stages in the hindbrain of a CNP-*lacZ* reporter mouse. CNP expression starts at E9.5 in the alar plate of rhombomeres 2, 4, and 6/7, where trigeminal, facial, vestibulocochlear, glossopharyngeal, and vagal sensory ax-

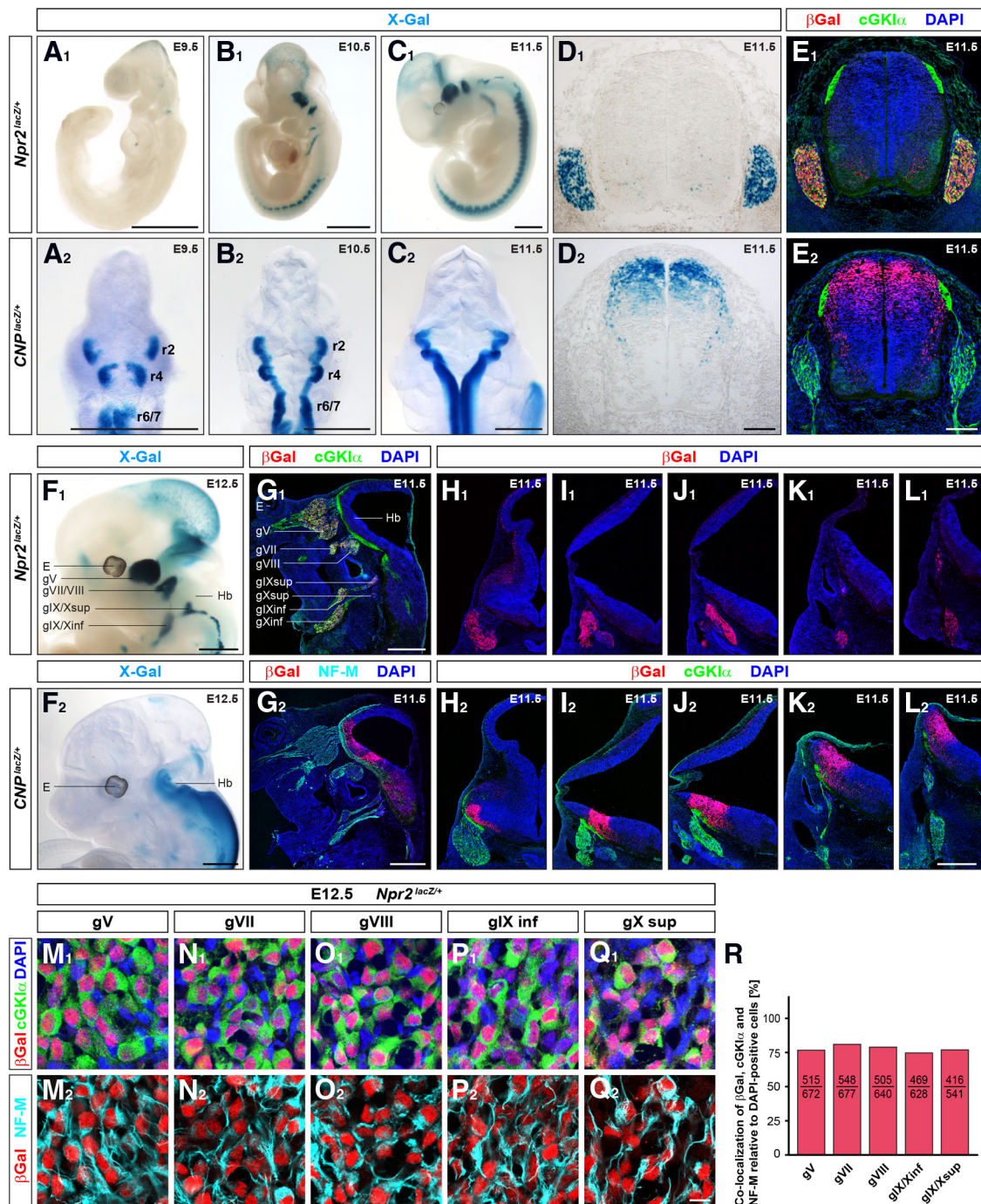


**Figure 2.** Complementary distribution of CNP in the hindbrain, and coexpression of Npr2 and cGKI $\alpha$  in cranial sensory neurons. **A<sub>1</sub>–D<sub>1</sub>**,  $\beta$ -gal activity in  $Npr2^{lacZ/+}$  whole-mount embryos (**A<sub>1</sub>–C<sub>1</sub>**) and in a transverse spinal cord section (**D<sub>1</sub>**) reveals sites of Npr2 expression at the indicated developmental stages. **A<sub>2</sub>–D<sub>2</sub>**, Embryonic expression pattern of CNP. X-gal staining represents the localization of CNP at the indicated developmental stages in dorsal views of the head region of  $CNP^{lacZ/+}$  whole-mount embryos (**A<sub>2</sub>–C<sub>2</sub>**) and in a transverse spinal cord section (**D<sub>2</sub>**). **E<sub>1</sub>, E<sub>2</sub>**, Immunohistochemical detection of  $\beta$ -gal and cGKI $\alpha$  in transverse sections of the spinal cord in  $Npr2^{lacZ/+}$  or  $CNP^{lacZ/+}$  mice, respectively, documenting coexpression of Npr2 and cGKI $\alpha$  in DRG neurons and CNP in dorsal regions of the spinal cord. **F<sub>1</sub>, F<sub>2</sub>**, X-gal stainings of  $Npr2^{lacZ/+}$  whole-mount embryo preparations at E12.5 (**F<sub>1</sub>**; lateral view) show a strong expression of  $\alpha$ -Npr2 in all cranial sensory ganglia, while  $\beta$ -gal activity representing CNP expression in  $CNP^{lacZ/+}$  mice (**F<sub>2</sub>**) is complementarily localized in the hindbrain. **G–L**, This is confirmed by immunohistochemical detection of  $\beta$ -gal in parasagittal sections of the hindbrain region (**G<sub>1</sub>, G<sub>2</sub>**) and in matching pairs of serial transverse sections from E11.5  $Npr2^{lacZ/+}$  and  $CNP^{lacZ/+}$  embryos at the level of gV (**H<sub>1</sub>, H<sub>2</sub>**), gVII (**I<sub>1</sub>, I<sub>2</sub>**), gVIII (**J<sub>1</sub>, J<sub>2</sub>**), gIX (**K<sub>1</sub>, K<sub>2</sub>**), and gX (**L<sub>1</sub>, L<sub>2</sub>**). Coimmunostaining reveals an overlapping distribution of  $\beta$ -gal with cGKI $\alpha$  expression in the cranial sensory ganglia of the  $Npr2^{lacZ/+}$  reporter (**G<sub>1</sub>**), which corresponds to the area stained by an antibody against neurofilament-M in  $CNP^{lacZ/+}$  mice (**G<sub>2</sub>**). **H<sub>2</sub>–L<sub>2</sub>**, Sites of CNP expression in the hindbrain are directly opposed to the entry zones of ingrowing cranial sensory axons as detected by colabeling for cGKI $\alpha$ . **M–Q**, The neuronal identity of cells coexpressing Npr2 and cGKI $\alpha$  in the cranial sensory ganglia of  $Npr2^{lacZ/+}$  mice was demonstrated by immunohistochemistry using antibodies directed against  $\beta$ -gal and cGKI $\alpha$  (**M<sub>1</sub>–Q<sub>1</sub>**) or neurofilament-M (**M<sub>2</sub>–Q<sub>2</sub>**). **R**, Percentage of  $\beta$ -gal<sup>+</sup>/cGKI $\alpha$ <sup>+</sup>/neurofilament-M<sup>+</sup> in relation to DAPI<sup>+</sup> cells in the cranial sensory ganglia of  $Npr2^{lacZ/+}$  embryos at E12.5. Absolute numbers counted are indicated in the columns. Nuclei in **E** and **G–Q** were visualized by DAPI. E, Eye; g, ganglion; Hb, hindbrain; r, rhombomere. Scale bars: **A–C**, 1 mm; **D–E**, 100  $\mu$ m; **F–L**, 500  $\mu$ m; **M–Q**, 10  $\mu$ m.

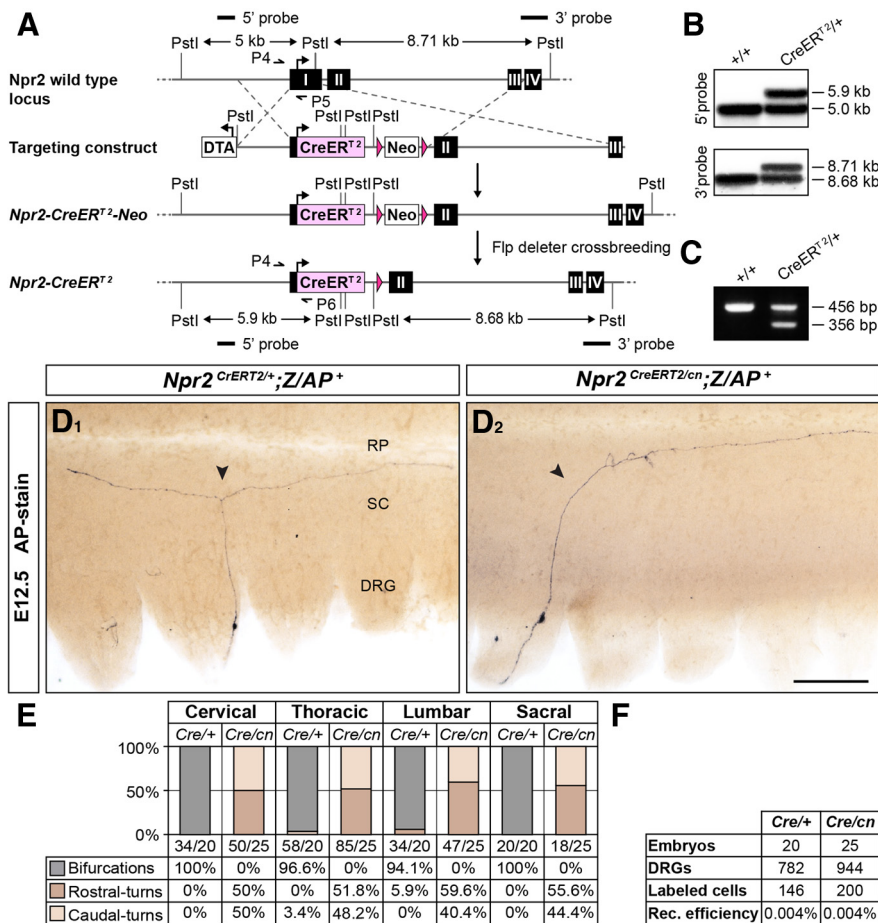


**Figure 3.** The *Npr2-CreER<sup>2</sup>* mouse line crossed to a reporter line enables the visualization of individual *Npr2*-expressing neurons. **A**, Targeting strategy for the generation of the *Npr2-CreER<sup>2</sup>* mouse line. **B**, **C**, Southern blot (**B**) and PCR genotyping (**C**) of wild-type and *Npr2<sup>CreER2/+</sup>* mice. **D**, Representative examples of alkaline phosphatase-stained DRG neurons in whole-mount spinal cord preparations from *Npr2<sup>CreER2/+</sup>;Z/AP<sup>+</sup>* and *Npr2<sup>CreER2/cn</sup>;Z/AP<sup>+</sup>* mice demonstrate a loss of axon bifurcation of DRG neurons in the spinal cord in *Npr2*-deficient animals. **E**, Quantification of the bifurcation behavior of DRG neurons from *Npr2* heterozygous (*Cre/+*) and homozygous deficient (*Cre/cn*) embryos. Total numbers of counted axons and numbers of analyzed embryos are indicated below the columns. **F**, Efficiency of the tamoxifen-induced recombination of the AP reporter construct in DRG neurons from *Npr2<sup>CreER2/+</sup>;Z/AP<sup>+</sup>* and *Npr2<sup>CreER2/cn</sup>;Z/AP<sup>+</sup>* mice. RP, Roof plate; SC, spinal cord. Scale bar: **D**, 250  $\mu$ m.

ons enter the hindbrain (Fig. 2A<sub>2</sub>–C<sub>2</sub>, F<sub>2</sub>–L<sub>2</sub>). As development proceeds, the structures between rhombomeres 2, 4, and 6/7 and more caudal parts of the hindbrain as well as the dorsal spinal cord also become strongly positive for CNP (Fig. 2C<sub>2</sub>–E<sub>2</sub>). At these early developmental stages, CNP is not found in the cranial sensory ganglia or DRGs (Fig. 2A<sub>2</sub>–E<sub>2</sub>).

Together, the expression of *Npr2* and *cGKI $\alpha$*  in all neurons of the cranial sensory ganglia and the complementary localization of CNP in the hindbrain suggest a function of *Npr2*-induced cGMP signaling for ingrowing cranial sensory axons.

**Analysis of axonal arborization of *Npr2*-expressing neurons by sparse transgenic labeling**

The investigation of the impact of *Npr2*-mediated cGMP signaling on axonal branching of cranial sensory neurons requires the visualization of individual axons. While axon tracing by DiI is a versatile and fast method for the analysis of axonal branching in DRG neurons, its application to the small cranial sensory ganglia, such as the jugular or nodose ganglia at early developmental stages, would be challenging. We therefore applied a genetic strategy for sparse labeling of *Npr2*-expressing neurons involving the generation of a mutant encoding a tamoxifen-inducible vari-

ant of Cre recombinase under control of the *Npr2* promoter (*Npr2-CreER<sup>2</sup>*; Fig. 3A; Feil et al., 1996). Southern blot and PCR analysis confirmed correct integration of the target vector (Fig. 3B, C). To validate the genetic strategy for the analysis of axon bifurcation, we compared the branching patterns of DRG neurons within the embryonic spinal cord of *Npr2* heterozygous mice, which resemble the wild-type phenotype (Schmidt et al., 2007), with those of homozygous *Npr2*-deficient animals. Tamoxifen-dependent activation of Cre recombinase in mouse embryos resulting from crossbreeding of heterozygous *Npr2-CreER<sup>2</sup>* mice with mice double-transgenic for the spontaneous loss-of-function mutation *Npr2-cn* and a conditional reporter allele (*Z/AP* or *tau-mGFP*; Lobe et al., 1999; Hippenmeyer et al., 2005) released reporter gene expression in the genetically defined subset of *Npr2*-expressing cells (Fig. 3D; Schmidt et al., 2013). In line with previous findings (Schmidt et al., 2007), we observed that 97.3% of the 146 AP-positive DRG neurons of *Npr2* heterozygous embryos showed a bifurcation of their central axons, whereas in the absence of *Npr2* activity all DRG axons (200 AP-positive neurons) revealed only turns and no bifurcation (Fig. 3E). Only axons that could be traced back to a cell soma in DRG were counted. No reporter activity was detected in the absence of tamoxifen. Assuming an average of 5000 neurons per DRG, a recombination frequency of 0.004% was calculated for the *Z/AP* system (Fig. 3F), which is in good approximation with earlier reports (Badea et al., 2009).

**Axons of cranial sensory neurons fail to bifurcate in *Npr2*-deficient mice**

After validation of the *Npr2-CreER<sup>2</sup>* mouse model as a useful tool to visualize axonal branching of *Npr2*-positive neurons, we studied the central projections of cranial sensory axons using the reporter lines *Z/AP* or *tau-mGFP*. Figure 4 shows examples of cranial sensory axons (79 of 82 axons visualized) that bifurcate in an ascending and a descending arm when *Npr2* is present. In contrast, in the absence of *Npr2* activity, all 163 visualized axons from the different cranial sensory ganglia turned without bifurcation in a descending or ascending stem axon (Fig. 4A–D, G, H). In addition to the bifurcation error, we occasionally observed aberrant cranial sensory axon projections at the entry zone, as illustrated for an axon from gIX (Fig. 4F). This axon turned in ascending direction but then looped backward and grew into the opposite direction. Similar observations have been occasionally made for DRG axons in the absence of *Npr2* (Schmidt et al., 2007).

Bifurcation of sensory axons at the entry zone of the brainstem results in the formation of two axon branches that ascend and descend in the ventrolateral region of the hindbrain. A lack of bifurcation at the entry zone, as observed in *Npr2* mutants, should thus evoke a significant reduction of axon numbers in the lateral hindbrain (see Fig. 8, scheme). As a

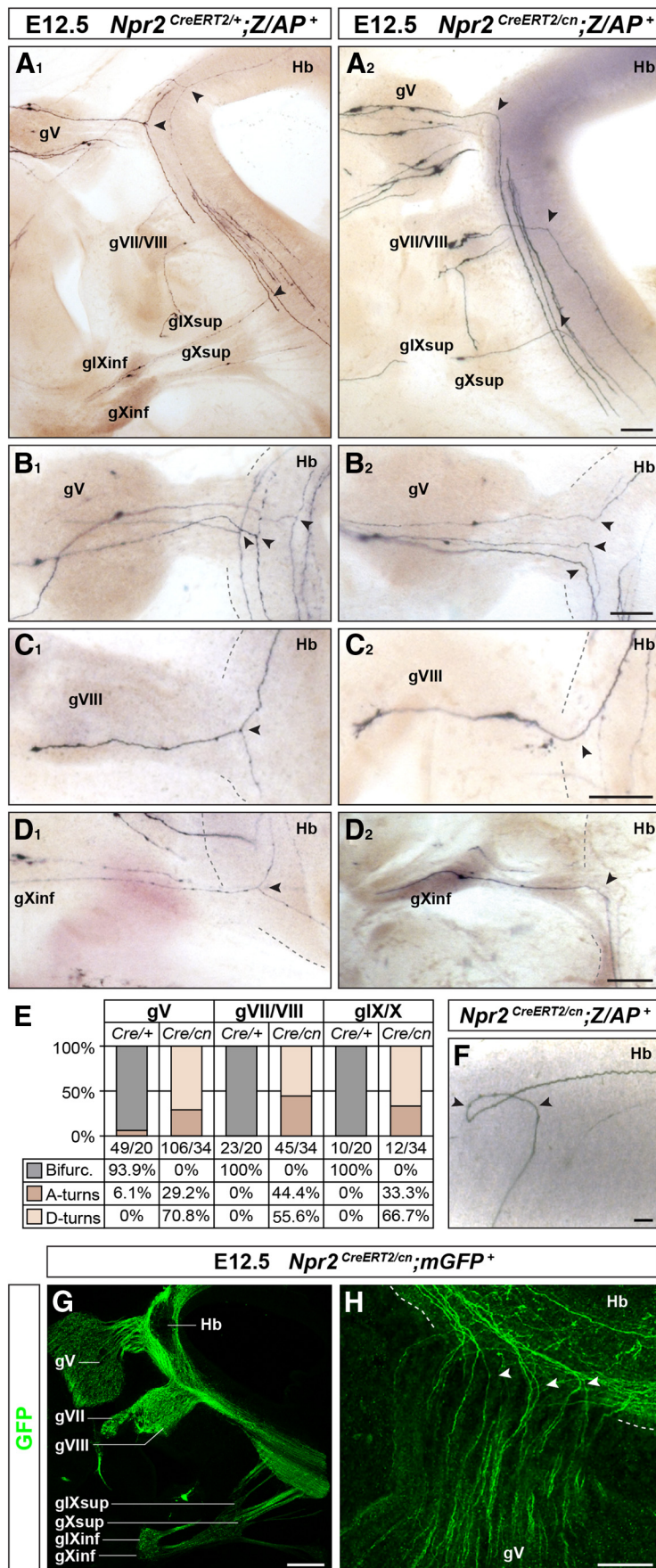


**Figure 4.** Bifurcation of axons from cranial sensory neurons depends on *Npr2*. **A–D**, AP staining of matched pairs of parasagittal sections from tamoxifen-treated *Npr2<sup>CreERT2/+</sup>;Z/AP<sup>+</sup>* and *Npr2<sup>CreERT2/cn</sup>;Z/AP<sup>+</sup>* mice demonstrates a loss of axon bifurcation in

measure of axon number, the area of anti-cGKI $\alpha$  immunoreactivity was quantified in cross sections of the hind-brain at the level of the trigeminal nerve. The cGKI $\alpha$ -labeled area in the trigeminal entry zone of E12.5 embryos amounted to 50% of wild-type controls in the absence of *Npr2* activity (Fig. 5*A, B*). This method only gives an indirect estimate of axon number; however, the measurements strongly suggest that, in mice lacking bifurcation in the entry zone of rhombomere 2, such zones contain substantially fewer sensory axon arms within the trigeminal entry region of the hindbrain, and this lack of sensory axon arms is not caused by an increase in the number of apoptotic cells (Fig. 5*C, D*).

To study whether CNP and cGKI $\alpha$ , the two other known components of the cGMP cascade that controls axon bifurcation of DRG neurons, also influence the bifurcation of cranial sensory neurons, we performed Dil tracing for trigeminal axons in CNP and cGKI mutant mice. This analysis demonstrated bifurcation errors at the hindbrain for CNP and cGKI knock-outs, indicating that these two components together with *Npr2* act in a signaling cascade that regulates branching of cranial sensory neurons (Fig. 6*A, B*).

**Collateral formation of axons from cranial sensory ganglia is not impaired in the absence of *Npr2***

After bifurcation, the two arms of the stem axons further branch out by generating collaterals at the axon shafts. Analysis of the *Z/AP* reporter mouse at more advanced embryonic stages revealed that

the central projection of cranial sensory neurons. **E**, Quantification of the bifurcation behavior of cranial sensory neurons from *Npr2* heterozygous (*Cre/+*) and homozygous deficient (*Cre/cn*) embryos. Total numbers of counted axons and numbers of analyzed embryos are indicated. **F**, AP-labeling of a parasagittal section from an E12.5 *Npr2<sup>CreERT2/cn</sup>;Z/AP<sup>+</sup>* embryo whose mother received tamoxifen at E9.5 shows an example of occasionally observed directionally aberrant turning behavior. Without bifurcating, a central axon from gIX first turned in an ascending direction and then looped backwards in the hindbrain. **G–H**, Anti-GFP immunostaining of cryosections of E12.5 *Npr2<sup>CreERT2/cn</sup>;mGFP<sup>+</sup>* embryos whose mothers received 4-hydroxytamoxifen at E9.5 indicates Cre-induced recombination in *Npr2*-expressing cells. In parasagittal sections of the hindbrain area, GFP-immunoreactivity is detected in all cranial sensory ganglia and their axonal projections (**G**). Higher magnification reveals trigeminal axons that fail to bifurcate in the hindbrain (**H**). The broken line indicates the border of the hindbrain and arrowheads show nonbifurcating trigeminal axons. g, Ganglion; Hb, hindbrain. Scale bars: **A**, 200  $\mu$ m; **B–D**, 100  $\mu$ m; **F**, 50  $\mu$ m; **G**, 250  $\mu$ m; **H**, 100  $\mu$ m.

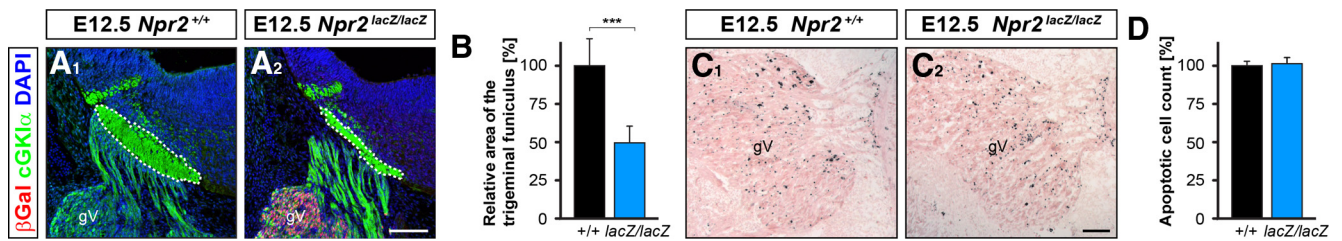


**Figure 5.** *A*, cGKI $\alpha$  immunostaining reveals a reduction in the size of the trigeminal funiculus (outlined by broken lines) in *Npr2*<sup>lacZ/lacZ</sup> mice. *B*, Quantification of the relative cGKI $\alpha$ -positive area of the developing trigeminal funiculus in transverse sections of wild-type and *Npr2* knock-out embryos (at least  $n = 60$  sections were analyzed from 3 embryos of each genotype).  $p < 0.001$ , Mann–Whitney  $U$  test. Error bars represent SD. *C*, *D*, TUNEL-detection (*C*) and quantification (*D*) of apoptotic cells in trigeminal ganglia at E12.5 in control and *Npr2*<sup>lacZ/lacZ</sup> mice. Error bars represent SE. Scale bars: *A*, *C*, 100  $\mu$ m.

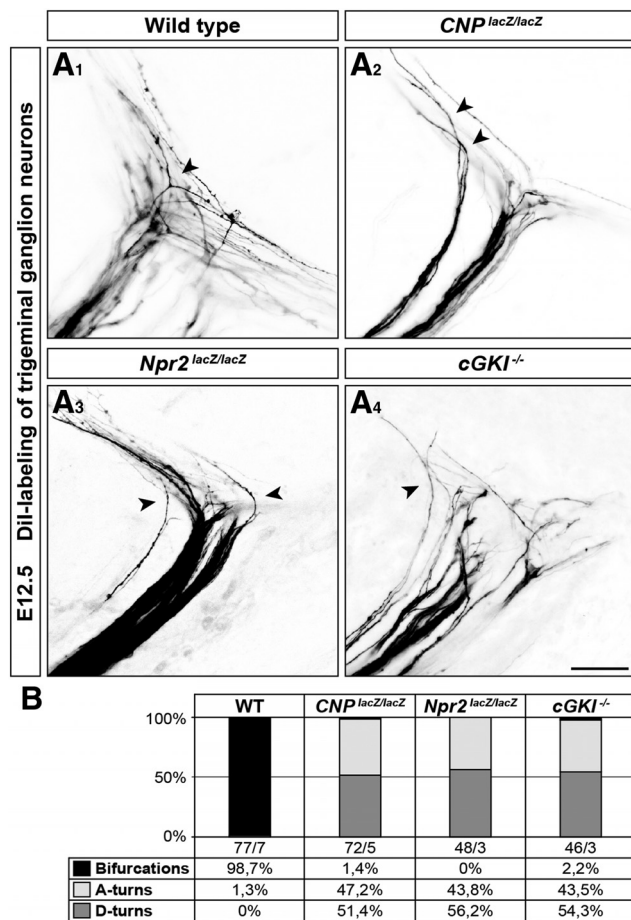


**Figure 6.** CNP-induced cGMP signaling triggers the bifurcation of central axons from trigeminal ganglion neurons in the hindbrain. *A*, Dil tracing of axon projections in parasagittal sections from wild-type (*A*<sub>1</sub>), *CNP*<sup>lacZ/lacZ</sup> (*A*<sub>2</sub>), *Npr2*<sup>lacZ/lacZ</sup> (*A*<sub>3</sub>), and *cGKI*<sup>-/-</sup> (*A*<sub>4</sub>) mice at E12.5. Axons from mice deficient for any of the components of the CNP-induced cGMP signaling pathway fail to bifurcate at the hindbrain. *B*, Quantification of Dil analysis showing the percentage of bifurcating, only ascending, or only descending trigeminal axons in the indicated genotypes. The numbers of single axons counted and analyzed embryos are given for each genotype. Scale bar, 50  $\mu$ m.

the formation of collaterals by cranial sensory axons was not impaired in the absence of *Npr2* activity (Fig. 7*A, B*). It is important to note that the inactivation of cGMP signaling via *Npr2* did not destroy the overall organization of the hindbrain or the formation of L1-positive axon tracts (Fig. 7*C–G*). In addition, no gross alterations in the peripheral processes of the ophthalmic branch of the trigeminal nerve in the absence of *Npr2* were observed in whole mounts of the head region as detected by anti-L1

staining (Fig. 7*H*), which is consistent with our observations on DRG axons (Schmidt et al., 2007).

In summary, axonal bifurcation of neurons from cranial sensory ganglia and DRGs is mediated in an analogous manner by *Npr2*-induced cGMP signaling.

### Discussion

During the course of target-directed navigation, axons form branches at specific points either through activities of their growth cone or in the axon shaft. Axonal branching is essential for the development of a functional nervous system. It allows an individual neuron to communicate with multiple neurons. Interstitial branching at the axon shaft appears to be the dominating branching mode in the brain and often occurs after growth of the primary axon, as has been observed for corticospinal or sensory axons (Nakamura and O’Leary, 1989; Ozaki and Snider, 1997). Although axonal branching during development is of crucial importance for the functionality of the mature nervous system, our molecular understanding of this process is still limited (Schmidt and Rathjen, 2010; Gallo, 2011; Gibson and Ma, 2011; Lewis et al., 2013). Defining signaling mechanisms that regulate axonal branching is therefore important for our understanding of how the complex pattern of neuronal connections is shaped. In the past, we analyzed the branching of DRG axons entering the spinal cord, whereby we and others identified a cGMP-dependent signaling cascade essential for axonal bifurcation *in vivo* (Schmidt et al., 2002, 2007, 2009; Zhao and Ma, 2009; Zhao et al., 2009). In this study, it was our aim to extend these observations to other neuronal populations through the use of genetic tools that allowed the analysis of axon branching in the hindbrain.

Our main conclusions of this study are as follows (Fig. 8): (1) at early developmental stages we observed a strong colocalization of *Npr2* and cGKI $\alpha$  in cranial sensory neurons and, importantly, a complementary expression of the ligand CNP in rhombomeres 2, 4, and 6/7 of the hindbrain; (2) all neurofilament-positive neurons of cranial sensory ganglia as well as DRGs were found to express both *Npr2* and cGKI $\alpha$ ; (3) in the absence of *Npr2*-induced cGMP signaling, bifurcation of axons from cranial sensory ganglia was completely disabled, and turns only in one direction were observed; (4) the formation of interstitial collaterals that extend into the corresponding brainstem nuclei to form terminal arbors on second-order neurons was not impaired, indicating that other signaling systems are important for this type of branch formation; and (5) the overall pathfinding of *Npr2*-positive axons in the CNS as well as in the periphery was not affected in the absence of this type of cGMP signaling. These overall building principles of branching and of target innervation are similar to the pattern found in the spinal cord, where *Npr2*-

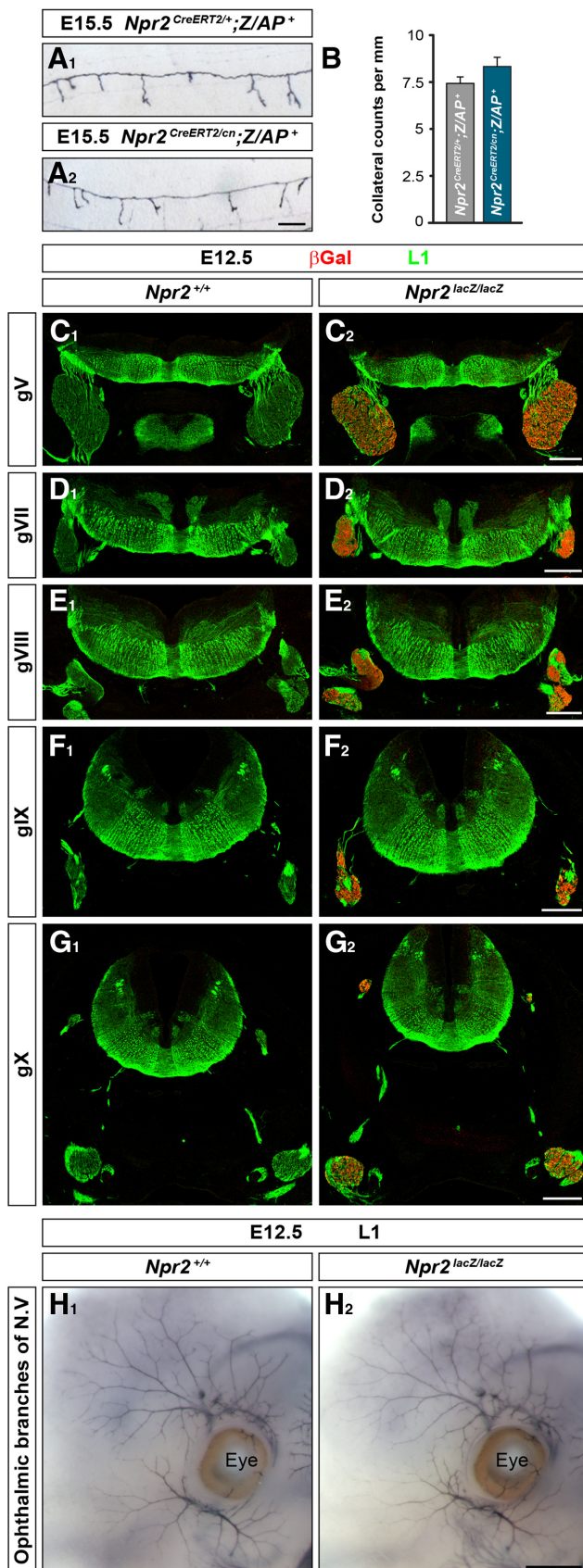


**Figure 7.** No alterations in collateral formation, in the overall pattern of embryonic hind-brain organization, or in trigeminal ophthalmic projections were observed in *Npr2*-deficient embryos. **A**, In both *Npr2<sup>CreERT2/+</sup>;Z/AP<sup>+</sup>* and *Npr2<sup>CreERT2/cn</sup>;Z/AP<sup>+</sup>* mice, collateral branches extend from the longitudinal axons of cranial sensory neurons in the hindbrain. **B**, Analysis of

induced cGMP signaling also mediates axonal bifurcation but not collateral formation or terminal branching.

Previously published tracing studies revealed that axons of several cranial ganglia bifurcate, thereby generating ascending and descending branches, which elongate along the lateral margin of the hindbrain. After a waiting period, interstitial collaterals are then generated from these stem axons that innervate their corresponding nuclear targets in the hindbrain, where they form terminal arbors on second-order neurons. For example, trigeminal collaterals terminate in the rostral principal nucleus and in the caudal spinal nucleus (Erzurumlu and Killackey, 1983; Erzurumlu and Jhaveri, 1992; Erzurumlu et al., 2010). Similarly, the axons of the bipolar neurons of the vestibular ganglion project to the ipsilateral hindbrain, where they bifurcate at the ventrolateral region of the lateral vestibular nucleus (Korte, 1979; Sato et al., 1989; McCue and Guinan, 1994; Imagawa et al., 1995, 1998; however, see also Maklad et al., 2010). Numerous collaterals are then elaborated. These terminate preferentially in the medial or superior vestibular nucleus (Sato et al., 1989; Maklad and Fritsch, 2002, 2003). Axons of the bipolar type I and pseudo-unipolar type II spiral ganglion cells, which are part of the VIII<sup>th</sup> cranial nerve, enter the brain, bifurcate, and form collaterals that innervate the subdivisions of the cochlear nucleus, the anteroventral cochlear nucleus, the posteroventral cochlear nucleus, and the dorsal cochlear nucleus (Fekete et al., 1984; Brown et al., 1988; Rubel and Fritsch, 2002; Ryugo and Parks, 2003; Koundakjian et al., 2007; Appler and Goodrich, 2011). Axons of the nodose ganglion, which belong to the vagus nerve, enter the hindbrain, bifurcate, and extend rostrocaudally within the solitary tract before they arborize within the ipsilateral nucleus of the solitary tract and spinal trigeminal nucleus (Rinaman and Levitt, 1993).

The nerves of cranial sensory ganglia also contain motor axons that run through or are closely associated with these ganglia. Standard tracing techniques using DiI, HRP, or Golgi silver impregnation are therefore exposed to the risk that motor axons, in addition to sensory axons, become labeled. This obvious handicap of traditional axon tracing methods might explain why earlier studies reported that a relatively large proportion of trigeminal axons enter the hindbrain without bifurcation (Windle, 1926; Hayashi, 1980; Tsuru et al., 1989). Our approach for transgenic labeling of *Npr2*-positive neurons circumvented this problem and enabled a reliable visualization of cranial sensory axon paths. For this purpose, we generated a driver mouse strain encoding a tamoxifen-inducible Cre recombinase under the promoter of *Npr2*, which was crossed with conditional reporter mice that contained floxed stop sequences upstream of the reporter allele. Expression of the reporter was only released after application of tamoxifen, which induced a transient activation and translocation of CreER<sup>T2</sup> into the nuclei of *Npr2*-positive cells. We applied two reporters: Z/AP or tau-mGFP. Axons were detected by AP activity or by GFP fluorescence. The use of the

collateral densities in *Npr2<sup>CreERT2/+</sup>;Z/AP<sup>+</sup>* and *Npr2<sup>CreERT2/cn</sup>;Z/AP<sup>+</sup>* mice. **C–G**, Matched pairs of transverse sections of E12.5 hindbrains from wild-type and *Npr2<sup>lacZ/lacZ</sup>* mice were stained with an antibody against L1 to reveal the gross anatomical organization of the hindbrain at the level of the different cranial sensory ganglia. As expected,  $\beta$ -gal was only detected in transgenic mice. **H**, Whole-mount anti-L1 immunostaining indicates no major differences between *Npr2<sup>lacZ/lacZ</sup>* animals and their wild-type littermate controls in the trigeminal ophthalmic projections surrounding the eye. Scale bars: **A**, 100  $\mu$ m; **C–G**, 250  $\mu$ m; **H**, 500  $\mu$ m.

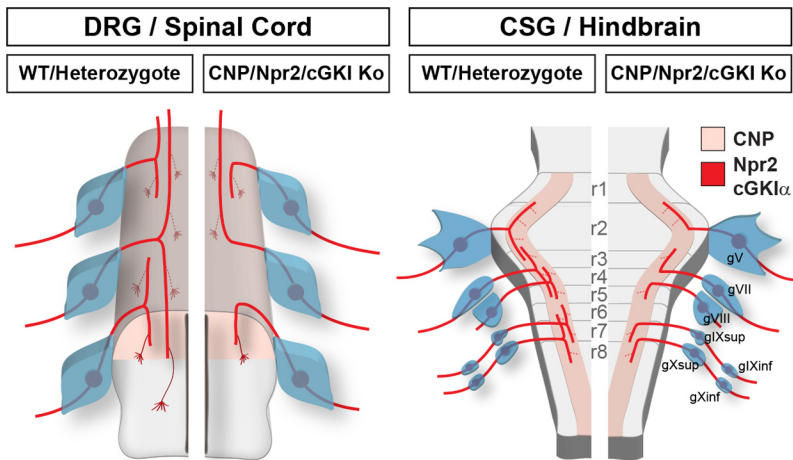


**Figure 8.** Schematic summary of the bifurcation defect observed in the absence of Npr2-induced cGMP-signaling in neurons of both DRG and cranial sensory ganglia. The localization of CNP, Npr2, and cGKI $\alpha$  are indicated. CSG, Cranial sensory ganglia; r1–r8, rhombomeres 1–8.

Z/AP reporter resulted in very low recombination frequencies, which facilitated the analysis of the paths of single axons in slice preparations. In contrast, the tau-mGFP reporter revealed a much higher frequency and the analysis of the trajectory of a single axon was only possible in stacks of confocal images. Both methods permitted a comprehensive and systematic analysis of axonal branching in the hindbrain at very early stages and demonstrated that all cranial Npr2 and neurofilament-positive sensory axons bifurcate in heterozygotes (corresponding to the wild-type situation). In the absence of Npr2-induced cGMP signaling, sensory axons only turn in one direction. DiI tracing experiments on the trigeminal ganglion in the absence of CNP, Npr2, or cGKI further support the notion that these three cGMP signaling components that were identified to be important for axonal branching in DRG neurons also control branching of cranial sensory neurons. In addition, a recently published study on DiI tracing of the VIII<sup>th</sup> nerve in *Npr2<sup>cn/cn</sup>* mice also supports our overall conclusions (Lu et al., 2011). In contrast, collateral formation is not impaired in the absence of Npr2-induced cGMP signaling, which is consistent with our view that distinct signaling cascades already exist in a single neuron to regulate distinct branching modes.

The cranial sensory ganglia contain neurons that transmit sensory information to the CNS. In contrast to the DRG neurons of the trunk, a substantial portion of the cranial sensory nervous system largely arises from specialized ectoderm—the sensory placodes—as well as from neural crest cells (D’Amico-Martel and Noden, 1983; Barlow, 2002; Lleras-Forero and Streit, 2012). This is exemplified by the trigeminal ganglion, which derives both from ectodermal placodes and neural crest cells migrating at the level of rhombomeres 1 and 2. The neurons of the inner ear, which transmit sound and the perception of rotational movements and accelerations to the brain, arise from the otic placode (Ladher et al., 2010). The petrosal placode contributes to the ninth cranial nerve (glossopharyngeal nerve), which innervates the tongue and the carotid sinus. The nodose placode contributes to the tenth cranial nerve (the vagus nerve), which detects sensory information from almost all of the organs in the body and is implicated in the regulation of cardiovascular, respiratory, gastrointestinal, and endocrine functions (Ratcliffe et al., 2011).

Behavioral studies aimed to understand why a T-shaped branching is of benefit for vertebrates to represent sensory information to the second-order neurons in the hindbrain or spinal cord are currently prevented by the postnatal lethality of global knock-outs for CNP, Npr2, or cGKI. In addition, the absence of CNP or Npr2, or mutations in CNP or Npr2, also impair long bone growth in mice and human patients, resulting in dwarf statures or overgrowth (Potter et al., 2009; Potter, 2011; Ter-Avetisyan et al., 2012). Further research requires additional mouse models that allow selective inactivation of the Npr2 signaling system in specific sensory ganglia.

Our study extends our initial observation of a cGMP signaling pathway that controls axonal bifurcation of DRG neurons to the population of cranial

sensory neurons and therefore suggests a more common function of Npr2-induced cGMP signaling for axonal branching. Interestingly, at more advanced developmental stages, several other neuronal subpopulations in the brain are found to be positive for Npr2 and cGKI $\alpha$ , including subpopulations in the cerebellum, hippocampus, and thalamus. However, the second messenger cGMP is implicated in several developmental and physiological processes in which cGMP signaling components are organized and function in different combinations (Lucas et al., 2000; Hofmann et al., 2006). A careful histological analysis of the localization of cGMP signaling components is therefore required before axonal branching studies are performed on these neuronal subpopulations. The genetic tools presented in this study provide helpful tools for the analysis of axonal branching of additional neuronal populations in the developing brain.

## References

- Appler JM, Goodrich LV (2011) Connecting the ear to the brain: Molecular mechanisms of auditory circuit assembly. *Prog Neurobiol* 93:488–508. [CrossRef Medline](#)
- Badea TC, Hua ZL, Smallwood PM, Williams J, Rotolo T, Ye X, Nathans J (2009) New mouse lines for the analysis of neuronal morphology using CreER(T)/loxP-directed sparse labeling. *PLoS One* 4:e7859. [CrossRef Medline](#)
- Barlow LA (2002) Cranial nerve development: placodal neurons ride the crest. *Curr Biol* 12:R171–R173. [CrossRef Medline](#)
- Brown AG (1981) Organization in the spinal cord. Berlin: Springer.
- Brown MC, Berglund AM, Kiang NY, Ryugo DK (1988) Central trajectories of type II spiral ganglion neurons. *J Comp Neurol* 278:581–590. [CrossRef Medline](#)
- D’Amico-Martel A, Noden DM (1983) Contributions of placodal and neural crest cells to avian cranial peripheral ganglia. *Am J Anat* 166:445–468. [CrossRef Medline](#)
- Erzurumlu RS, Jhaveri S (1992) Trigeminal ganglion cell processes are spatially ordered prior to the differentiation of the vibrissa pad. *J Neurosci* 12:3946–3955. [Medline](#)
- Erzurumlu RS, Killackey HP (1983) Development of order in the rat trigeminal system. *J Comp Neurol* 213:365–380. [CrossRef Medline](#)
- Erzurumlu RS, Murakami Y, Rijli FM (2010) Mapping the face in the somatosensory brainstem. *Nat Rev Neurosci* 11:252–263. [CrossRef Medline](#)
- Feil R, Brocard J, Mascrez B, LeMeur M, Metzger D, Chambon P (1996) Ligand-activated site-specific recombination in mice. *Proc Natl Acad Sci U S A* 93:10887–10890. [CrossRef Medline](#)
- Feil R, Wagner J, Metzger D, Chambon P (1997) Regulation of Cre recom-

- binase activity by mutated estrogen receptor ligand-binding domains. *Biochem Biophys Res Commun* 237:752–757. [CrossRef Medline](#)
- Fekete DM, Rouiller EM, Liberman MC, Ryugo DK (1984) The central projections of intracellularly labeled auditory nerve fibers in cats. *J Comp Neurol* 229:432–450. [CrossRef Medline](#)
- Gallo G (2011) The cytoskeletal and signaling mechanisms of axon collateral branching. *Dev Neurobiol* 71:201–220. [CrossRef Medline](#)
- Geister KA, Brinkmeier ML, Hsieh M, Faust SM, Karolyi JJ, Perosky JE, Kozloff KM, Conti M, Camper SA (2013) A novel loss-of-function mutation in *Npr2* clarifies primary role in female reproduction and reveals a potential therapy for acromesomelic dysplasia, Maroteaux type. *Hum Mol Genet* 22:345–357. [CrossRef Medline](#)
- Gibson DA, Ma L (2011) Developmental regulation of axon branching in the vertebrate nervous system. *Development* 138:183–195. [CrossRef Medline](#)
- Hama H, Kurokawa H, Kawano H, Ando R, Shimogori T, Noda H, Fukami K, Sakaue-Sawano A, Miyawaki A (2011) Scale: a chemical approach for fluorescence imaging and reconstruction of transparent mouse brain. *Nat Neurosci* 14:1481–1488. [CrossRef Medline](#)
- Hayashi H (1980) Distributions of vibrissae afferent fiber collaterals in the trigeminal nuclei as revealed by intra-axonal injection of horseradish peroxidase. *Brain Res* 183:442–446. [CrossRef Medline](#)
- Hippenmeyer S, Vrieseling E, Sigrist M, Portmann T, Laengle C, Ladle DR, Arber S (2005) A developmental switch in the response of DRG neurons to ETS transcription factor signaling. *PLoS Biol* 3:e159. [CrossRef Medline](#)
- Hofmann F, Feil R, Kleppisch T, Schlossmann J (2006) Function of cGMP-dependent protein kinases as revealed by gene deletion. *Physiol Rev* 86:1–23. [CrossRef Medline](#)
- Imagawa M, Isu N, Sasaki M, Endo K, Ikegami H, Uchino Y (1995) Axonal projections of utricular afferents to the vestibular nuclei and the abducens nucleus in cats. *Neurosci Lett* 186:87–90. [CrossRef Medline](#)
- Imagawa M, Graf W, Sato H, Suwa H, Isu N, Izumi R, Uchino Y (1998) Morphology of single afferents of the saccular macula in cats. *Neurosci Lett* 240:127–130. [CrossRef Medline](#)
- Indra AK, Warot X, Brocard J, Bornert JM, Xiao JH, Chambon P, Metzger D (1999) Temporally controlled site-specific mutagenesis in the basal layer of the epidermis: comparison of the recombinase activity of the tamoxifen-inducible Cre-ER(T) and Cre-ER(T2) recombinases. *Nucleic Acids Res* 27:4324–4327. [CrossRef Medline](#)
- Joyner AL, Zervas M (2006) Genetic inducible fate mapping in mouse: establishing genetic lineages and defining genetic neuroanatomy in the nervous system. *Dev Dyn* 235:2376–2385. [CrossRef Medline](#)
- Korte GE (1979) The brainstem projection of the vestibular nerve in the cat. *J Comp Neurol* 184:279–292. [CrossRef Medline](#)
- Koundakjian EJ, Appller JL, Goodrich LV (2007) Auditory neurons make stereotyped wiring decisions before maturation of their targets. *J Neurosci* 27:14078–14088. [CrossRef Medline](#)
- Ladher RK, O'Neill P, Begbie J (2010) From shared lineage to distinct functions: the development of the inner ear and epibranchial placodes. *Development* 137:1777–1785. [CrossRef Medline](#)
- Lee EC, Yu D, Martinez de Velasco L, Tessarollo L, Swing DA, Court DL, Jenkins NA, Copeland NG (2001) A highly efficient *Escherichia coli*-based chromosome engineering system adapted for recombinogenic targeting and subcloning of BAC DNA. *Genomics* 73:56–65. [CrossRef Medline](#)
- Lewis TL Jr, Courchet J, Polleux F (2013) Cell biology in neuroscience: cellular and molecular mechanisms underlying axon formation, growth, and branching. *J Cell Biol* 202:837–848. [CrossRef Medline](#)
- Lilley BN, Pan YA, Sanes JR (2013) SAD kinases sculpt axonal arbors of sensory neurons through long- and short-term responses to neurotrophin signals. *Neuron* 79:39–53. [CrossRef Medline](#)
- Lleras-Forero L, Streit A (2012) Development of the sensory nervous system in the vertebrate head: the importance of being on time. *Curr Opin Genet Dev* 22:315–322. [CrossRef Medline](#)
- Lobe CG, Koop KE, Kreppner W, Lomeli H, Gertsenstein M, Nagy A (1999) Z/AP, a double reporter for cre-mediated recombination. *Dev Biol* 208:281–292. [CrossRef Medline](#)
- Lu CC, Appller JM, Houseman EA, Goodrich LV (2011) Developmental profiling of spiral ganglion neurons reveals insights into auditory circuit assembly. *J Neurosci* 31:10903–10918. [CrossRef Medline](#)
- Lucas KA, Pitari GM, Kazerounian S, Ruiz-Stewart I, Park J, Schulz S, Chepenik KP, Waldman SA (2000) Guanylyl cyclases and signaling by cyclic GMP. *Pharmacol Rev* 52:375–414. [Medline](#)
- Maklad A, Fritsch B (2002) The developmental segregation of posterior crista and saccular vestibular fibers in mice: a carbocyanine tracer study using confocal microscopy. *Brain Res Dev Brain Res* 135:1–17. [CrossRef Medline](#)
- Maklad A, Fritsch B (2003) Development of vestibular afferent projections into the hindbrain and their central targets. *Brain Res Bull* 60:497–510. [CrossRef Medline](#)
- Maklad A, Kamel S, Wong E, Fritsch B (2010) Development and organization of polarity-specific segregation of primary vestibular afferent fibers in mice. *Cell Tissue Res* 340:303–321. [CrossRef Medline](#)
- McCue MP, Guinan JJ Jr (1994) Acoustically responsive fibers in the vestibular nerve of the cat. *J Neurosci* 14:6058–6070. [Medline](#)
- Nakamura H, O'Leary DD (1989) Inaccuracies in initial growth and arborization of chick retinotectal axons followed by course corrections and axon remodeling to develop topographic order. *J Neurosci* 9:3776–3795. [Medline](#)
- Ozaki S, Snider WD (1997) Initial trajectories of sensory axons toward laminar targets in the developing mouse spinal cord. *J Comp Neurol* 380:215–229. [CrossRef Medline](#)
- Potter LR (2011) Guanylyl cyclase structure, function and regulation. *Cell Signal* 23:1921–1926. [CrossRef Medline](#)
- Potter LR, Yoder AR, Flora DR, Antos LK, Dickey DM (2009) Natriuretic peptides: their structures, receptors, physiologic functions and therapeutic applications. *Handb Exp Pharmacol* 191:341–366. [CrossRef Medline](#)
- Ratcliffe EM, Farrar NR, Fox EA (2011) Development of the vagal innervation of the gut: steering the wandering nerve. *Neurogastroenterol Motil* 23:898–911. [CrossRef Medline](#)
- Rathjen FG, Schachner M (1984) Immunocytological and biochemical characterization of a new neuronal cell surface component (L1 antigen) which is involved in cell adhesion. *EMBO J* 3:1–10. [Medline](#)
- Rinaman L, Levitt P (1993) Establishment of vagal sensorimotor circuits during fetal development in rats. *J Neurobiol* 24:641–659. [CrossRef Medline](#)
- Rotolo T, Smallwood PM, Williams J, Nathans J (2008) Genetically-directed, cell type-specific sparse labeling for the analysis of neuronal morphology. *PLoS One* 3:e4099. [CrossRef Medline](#)
- Rubel EW, Fritsch B (2002) Auditory system development: primary auditory neurons and their targets. *Annu Rev Neurosci* 25:51–101. [CrossRef Medline](#)
- Ryugo DK, Parks TN (2003) Primary innervation of the avian and mammalian cochlear nucleus. *Brain Res Bull* 60:435–456. [CrossRef Medline](#)
- Sato F, Sasaki H, Ishizuka N, Sasaki S, Mannen H (1989) Morphology of single primary vestibular afferents originating from the horizontal semicircular canal in the cat. *J Comp Neurol* 290:423–439. [CrossRef Medline](#)
- Schmidt H, Rathjen FG (2010) Signalling mechanisms regulating axonal branching *in vivo*. *Bioessays* 32:977–985. [CrossRef Medline](#)
- Schmidt H, Rathjen FG (2011) DiI-labeling of DRG neurons to study axonal branching in a whole mount preparation of mouse embryonic spinal cord. *J Vis Exp pii:3667* [CrossRef Medline](#)
- Schmidt H, Werner M, Heppenstall PA, Henning M, Moré MI, Kühbandner S, Lewin GR, Hofmann F, Feil R, Rathjen FG (2002) cGMP-mediated signaling via cGK1alpha is required for the guidance and connectivity of sensory axons. *J Cell Biol* 159:489–498. [CrossRef Medline](#)
- Schmidt H, Stonkute A, Jüttner R, Schäffer S, Buttgerit J, Feil R, Hofmann F, Rathjen FG (2007) The receptor guanylyl cyclase *Npr2* is essential for sensory axon bifurcation within the spinal cord. *J Cell Biol* 179:331–340. [CrossRef Medline](#)
- Schmidt H, Stonkute A, Jüttner R, Koesling D, Friebe A, Rathjen FG (2009) C-type natriuretic peptide (CNP) is a bifurcation factor for sensory neurons. *Proc Natl Acad Sci U S A* 106:16847–16852. [CrossRef Medline](#)
- Schmidt H, Ter-Avetisyan G, Rathjen FG (2013) A genetic strategy for the analysis of individual axon morphologies in cGMP signalling mutant mice. *Methods Mol Biol* 1020:193–204. [CrossRef Medline](#)
- Stefanini M, De Martino C, Zamboni L (1967) Fixation of ejaculated spermatozoa for electron microscopy. *Nature* 216:173–174. [CrossRef Medline](#)
- Tamura N, Doolittle LK, Hammer RE, Shelton JM, Richardson JA, Garbers

- DL (2004) Critical roles of the guanylyl cyclase B receptor in endochondral ossification and development of female reproductive organs. *Proc Natl Acad Sci U S A* 101:17300–17305. [CrossRef Medline](#)
- Ter-Avetisyan G, Tröster P, Schmidt H, Rathjen FG (2012) cGMP signaling and branching of sensory axons in the spinal cord. *Fut Neurol* 7:639–651. [CrossRef](#)
- Tsuji T, Kunieda T (2005) A loss-of-function mutation in natriuretic peptide receptor 2 (*Npr2*) gene is responsible for disproportionate dwarfism in *cn/cn* mouse. *J Biol Chem* 280:14288–14292. [CrossRef Medline](#)
- Tsuru K, Otani K, Kajiyama K, Suemune S, Shigenaga Y (1989) Central terminations of periodontal mechanoreceptive and tooth pulp afferents in the trigeminal principal and oral nuclei of the cat. *Brain Res* 485:29–61. [CrossRef Medline](#)
- Wegener JW, Nawrath H, Wolfsgruber W, Kühbandner S, Werner C, Hofmann F, Feil R (2002) cGMP-dependent protein kinase I mediates the negative inotropic effect of cGMP in the murine myocardium. *Circ Res* 90:18–20. [CrossRef Medline](#)
- Windle WF (1926) Non-bifurcating nerve fibers of the trigeminal nerve. *J Comp Neurol* 40:229–240. [CrossRef](#)
- Zhao Z, Ma L (2009) Regulation of axonal development by natriuretic peptide hormones. *Proc Natl Acad Sci U S A* 106:18016–18021. [CrossRef Medline](#)
- Zhao Z, Wang Z, Gu Y, Feil R, Hofmann F, Ma L (2009) Regulate axon branching by the cyclic GMP pathway via inhibition of glycogen synthase kinase 3 in dorsal root ganglion sensory neurons. *J Neurosci* 29:1350–1360. [CrossRef Medline](#)